

# Computer simulation of the trajectories of large water jets

A. P. Hatton<sup>†</sup>, C. M. Leech<sup>†</sup> and M. J. Osborne\*

A three-dimensional computer simulation of the motion of a water jet is described which includes the effects of wind from any direction. The simulation is useful in the design of fire-fighting systems, particularly those used in offshore situations. The equations of motion are presented in vector form and the problem of the fluid dynamic drag variation is discussed. Semi-empirical approximations for the drag components along and across the jet are presented which involve four unknown constants. These are reduced to three by using previous data on the efficiency of vertical jets. To fix the remaining constants, information was available from a series of large jet tests carried out to prove an offshore fire fighting system. In these tests different nozzle shapes were tried and, using the best of these shapes, a large number of trajectories were measured photographically. These were used to fix the simulation drag constants and good agreement is shown between measurements and predictions. The simulation enables the effects of flow-rate, pressure, nozzle size, elevation and wind strength to be evaluated in the system design

**Keywords:** *fluid dynamics, sloshing frequencies, two-fluid systems, closed tanks*

With the proliferation of drilling and production platforms in the North Sea and other continental shelves, the fire hazard has become a subject of major importance in the offshore industry. Specialised craft for offshore fire fighting use large water jets and the object of this paper is to present a theoretical analysis of jet behaviour and to compare this with results obtained from a recent series of large jet tests.

## Previous work on water jets

While much work has been carried out on small fuel jets and on air jets, there is only limited work on large water jets. Freeman<sup>1</sup> tested a range of nozzles up to 2 in (50.8 mm) diameter using pressures up to 100 psig (6.8 bar) and measured discharge coefficients and trajectories. As a result of his tests he proposed the 'classical' fire nozzle profile. Rouse *et al.*<sup>2</sup> carried out intensive tests and proposed a new design of monitor and nozzle. The nozzle profile had a concave inner surface and convergent exit. Rouse tested jets up to 3 in (76.2 mm) diameter with pressures up to 200 psig (13.8 bar) but showed that there was little gain in range for jets of this size by increasing pressures above 150 psig (10 bar). Murakami and Katayama<sup>3</sup> measured discharge coefficients of a large number of nozzle-branch pipe combinations. Hoyt and Taylor<sup>4</sup> tested a number of nozzles of unusual shape but concluded that there was no clear advantage in any of the designs tested. A computer simulation of large jet be-

haviour was proposed by Hatton and Osborne<sup>5</sup> but this used a simple drag approximation of a constant drag coefficient along the jet, although the coefficient was a function of the initial Froude number. They based the drag approximation on vertical jet tests by Arato *et al.*<sup>6</sup> and any drag approximation must satisfy these tests. This article proposes improved drag formulations.

Recently a series of large jet tests were carried out at the British Ship Research Association Laboratory<sup>7</sup>. Jets up to 15.2 cm diameter were tested capable of 3600 m<sup>3</sup>/h capacity at pressures up to 14 bar.

Range was measured by photographing the jets against a surveyed background and trajectories were measured for flow rates of 1200, 2400 and 3600 m<sup>3</sup>/h for a range of elevations. The monitor incorporated a long tapering branch pipe of 5° cone angle with flow straighteners at both inlet and outlet. Fig 1 shows the types of nozzle tested. The results showed that the ranges

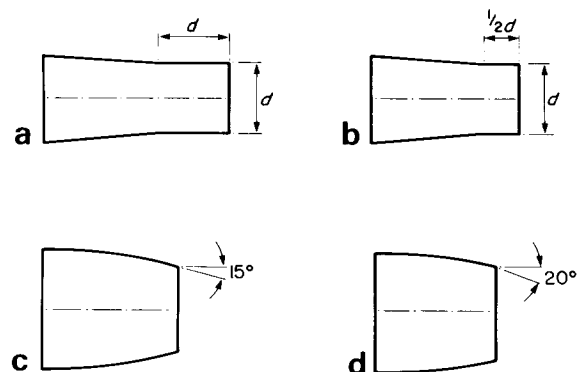


Fig 1 Typical shapes of nozzles used in trajectory tests

<sup>†</sup> Department of Mechanical Engineering, University of Manchester Institute of Science & Technology, PO Box 88, Manchester M60 1QD, UK

\* Fire Defence Services Ltd, Knutsford, Cheshire

Received 2 October 1984 and accepted for publication on 12 February 1985

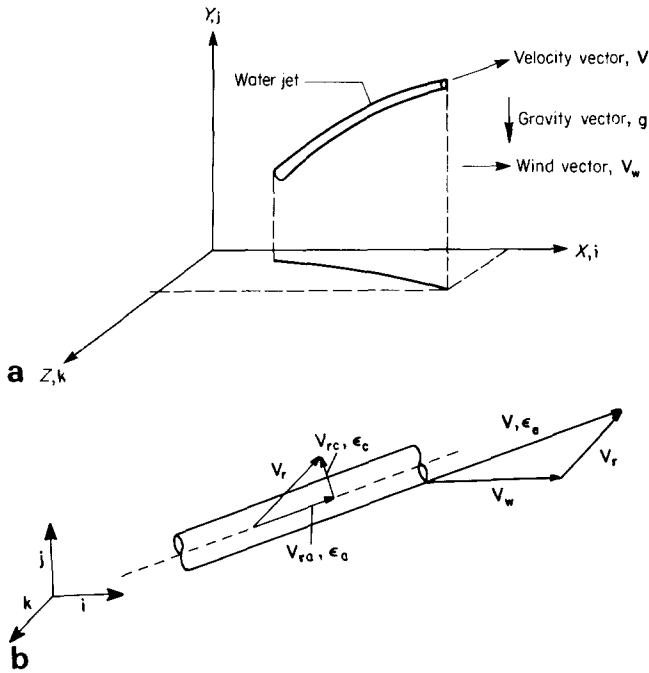


Fig 2 (a) Jet schematic and coordinates; (b) Vector diagram and representation of relative velocities

achieved by the Rouse type nozzles (Figs 1(c) and 1(d)) were rather less than the other types and that the coherence of the jets from the Rouse type nozzles was markedly worse than the other types. The best form of nozzle in these tests emerged as the type shown in Fig 1(b), namely a gradual convergence blending into a short parallel section. Results of the trajectory measurements are given later.

### Equations of motion of a jet

#### Dynamic equations

For the system shown in Fig 2, the dynamic equations are:

$$\dot{V} = -g - F$$

$$\dot{X} = V$$

$$\dot{S} = |V|$$

where:

$$V = (V_x, V_y, V_z)$$

$$g = (0, -g, 0)$$

$$F = (F_x, F_y, F_z)$$

$$X = (x, y, z)$$

The vector  $V$  is the velocity of a component of the jet at a time  $t$  after it has left the nozzle. The vector  $g$  is the gravitation vector and is shown to act in the  $-j$  direction. The  $F$  vector is the drag/unit mass, and as shown has components in the three axis directions. However, these components arise from consideration of a resolution along the jet and across it.

#### Drag components

If the unit vectors  $i, j, k$  are introduced, aligning themselves along the  $x, y$  and  $z$  axis system, then the velocity vector:

$$V = V_x i + V_y j + V_z k$$

Wind is similarly accounted for:

$$V_w = V_{wx} i + V_{wy} j + V_{wz} k$$

The relative air-velocity of the jet is then:

$$V_r = V - V_w$$

and the air speed along the jet can be written as:

$$V_{ra} = \frac{V_r \cdot V}{|V|} = V_r \cdot \epsilon_a$$

where  $\epsilon_a$  is the unit vector along the jet direction. The cross flow direction  $\epsilon_c$  can be obtained from:

$$\epsilon_c = \frac{(V_r \times \epsilon_a) \times \epsilon_a}{|V_r \times \epsilon_a|}$$

and the cross flow component is then:

$$V_{rc} = V_r \cdot \epsilon_c$$

The drag then depends on the directions of the tangential and cross flow forces, namely  $\epsilon_a$  and  $\epsilon_c$ , and the magnitudes of these forces as functions of the relative flows, namely  $V_{ra}$

Notation		X, Y	Empirical constants used to define the cross flow drag law
$C_D$	Drag coefficient, (drag force/ $v^2$ )	$\epsilon$	Unit vectors
$d$	Initial jet diameter	$\eta$	Jet efficiency (defined as the ratio of true height of a vertical jet to the head at the nozzle)
$F$	Drag force on the jet (vector)		
$Fr$	Froude number ( $V_0/\sqrt{gd}$ )		
$g$	Acceleration due to gravity		
$k, b, A, B, C$	Empirical constants used in defining the streamwise drag laws		
$S$	Distance along jet		
$t$	Time		
$V$	Velocity		
$X$	$x, y, z$ , coordinate vector position		
		<b>Subscripts</b>	
		a, c	Along and cross components
		r	Relative
		w	Wind
		x, y, z	Measured in Cartesian coordinate directions

and  $V_{rc}$ . Hence, the drag laws are functionally as follows:

$$F_a = f_a(V_{ra}, S)\epsilon_a$$

$$F_c = f_c(V_{rc}, S)\epsilon_c$$

where  $S$  is the distance along the jet. This parameter is included to account for jet swelling and break up.

These equations were solved on a CDC-CYBER 72 digital computer using the Runge-Kutta integration algorithm with step size control. The output utilises the graphics facility available on the CYBER (and full exploitation is made of the interactive facility available).

## Drag approximations

In the present state of knowledge it is not possible to calculate, from fundamental principles, the detailed motion and break up of a large water jet. We must, therefore, resort to empiricism using a logical approach and based on experimental measurements.

Hatton and Osborne<sup>6</sup> took the drag force along the jet direction as  $kV^2$ , typical of the format of turbulent flow drag over bluff bodies. This is clearly not satisfactory since the jet is steadily entraining air and disintegrating along its trajectory. In the early stages, the jet surface area is small and the drag force per unit of mass flow is correspondingly low. In the later stage as the jet becomes a cloud of droplets, the drag force will be large. There are various ways of attempting to describe this enhancement of drag coefficient with distance to obtain an improved simulation. It is necessary, however, to satisfy the requirement that any prediction will match the efficiency law of a vertical jet derived from the experimental data of Arato *et al.*<sup>6</sup>, namely for  $37 < Fr < 120$ :

$$\eta = 1.2294 - 0.007912Fr$$

where the Froude number is based on the nozzle diameter and exit velocity\*. This information enables one arbitrary constant in any drag expression to be fixed. For example if  $kV^2$  is chosen,  $k$  can be calculated to fit this data.

The expressions which were tried were:

$$(i) \text{ Drag Force} = kV^2(1 + AS + BS^2 + CS^n)$$

from which simpler forms could be extracted, for example by making certain constants zero.

$$(ii) \text{ Drag Force} = kV^2(1 + e^{bS}).$$

The exponential suggests itself since experience shows the very rapid deceleration of a jet as it disintegrates.

Turning now to the effects of cross winds, there appears to be no experimental information on the behaviour of large water jets in winds. For solid cylinders the cross component drag coefficient is much greater than the axial component drag coefficient (of the order of 50 times). In the early part of the flow the jet appears cylindrical so that the cross component coefficient might be considered as similar to that of a solid cylinder. In the later part of the flow the jet has dispersed into a cloud of droplets. It would be reasonable to assume that for such a cloud there would be no preferred direction and the cross drag coefficient will be the same as the axial coefficient.

\* It is interesting to note that as far as can be ascertained, the large Geneva fountain and that at Fountain Hill (Arizona) obey this expression.

To simulate this effect it was assumed that the cross drag coefficient would be an integer multiple  $X$  of the axial coefficient at the start and this would decay along the length of the jet until it became unity. This is achieved by the expression:

$$C_{Dc} = C_{Da}[(X - 1)e^{-YS} + 1]$$

where  $X$  and  $Y$  must be chosen to fit the data. If  $Y$  is zero, then the  $C_{Dc}$  remains equal to  $X \cdot C_{Da}$  along the jet. If  $Y$  is finite then when  $YS$  becomes large,  $C_{Dc}$  decays towards  $C_{Da}$ .

The computer program was written to include all the above features. A large number of runs were carried out to investigate the relative importance of the various choice parameters and comparisons made with the measured trajectories.

## Choice of drag approximation

The two drag coefficient approximations above contain too many choice parameters – four in (i) and two in (ii). However, a series of runs were made with both versions with the objective of achieving what appears to be representative of jet behaviour. For these calculations a nozzle diameter of 0.15 m, velocity 50 m/s and elevation 40° were chosen. These correspond to a flow rate of 3180 m<sup>3</sup>/h and nozzle pressure 12.5 bar (approximately). For example, Fig 3(a) shows four trajectories using drag force equal to  $kV^2(1 + AS)$  which is a form of (i). The values of  $A$  are 0.01, 0.05, 1.00 and 50. Very little effect is observed on the trajectory because the program uses the vertical jet efficiency first to find the value of  $k$ . Clearly this type of drag approximation is unrealistic because changes of the choice of  $A$  do not result in the types of trajectory shapes observed in practice. Further similar tests eventually showed that the format of (i) is too complex and it was abandoned in favour of format (ii). Fig 3(b) shows the results of the use of the format  $kV^2(1 + e^{bS})$  in which there is only one free parameter,  $b$ , and the values of  $b$  used are shown. This produces curves which are now typical of jet trajectories having the rapid fall in the later stages as the jet disintegrates and it was decided to adopt this format to fit the measured trajectories.

Having adopted the drag law  $kV^2(1 + e^{bS})$ , then the constant will result from matching the test trajectory with the predictions to obtain the most satisfactory value of  $b$ .

Fig 4(a) shows the simulation of a vertical jet in a cross wind. The four combinations of  $X$  and  $Y$  used are (50, 0.01), (50, 0.02), (50, 0.04) and (20, 0.02). It would appear that the choice of  $X$  does not have as strong an influence on the resulting jet motion as the choice of  $Y$ . With the choice of  $Y$  as 0.02 the value of the decay factor  $e^{-YS}$  is 0.37 at 50 m. For a choice of  $X$  of 50 this means that the across drag coefficient is reduced to approximately 18 times the along drag coefficient. There is no experimental data to support these values and they are used to illustrate the drift induced by cross winds.

Fig 4(b) shows some simulations of a large jet at 40° elevation in a cross wind of 10 m/s. Again the choices of  $X$  and  $Y$  show the strong influence of the  $Y$  choice with the smaller values of  $Y$  producing large deflection.

## Validation of the simulation constants

The extensive series of tests at the British Ship Research Association Laboratories<sup>1</sup> provided considerable

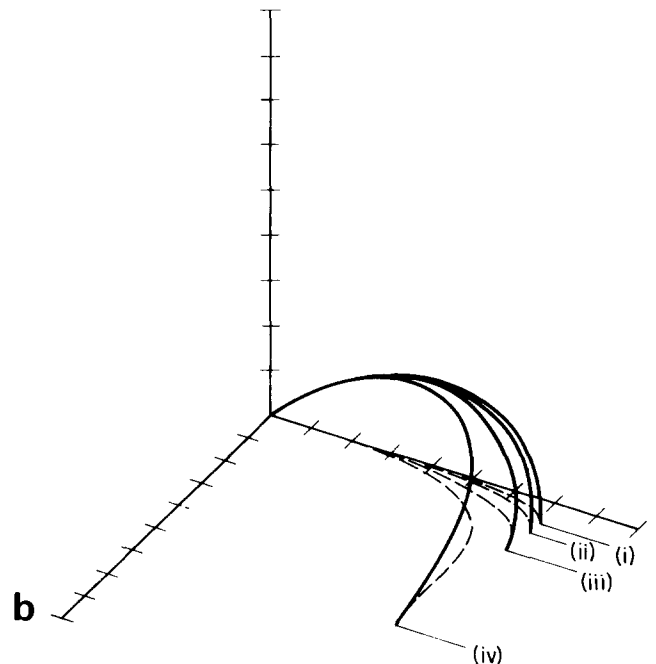
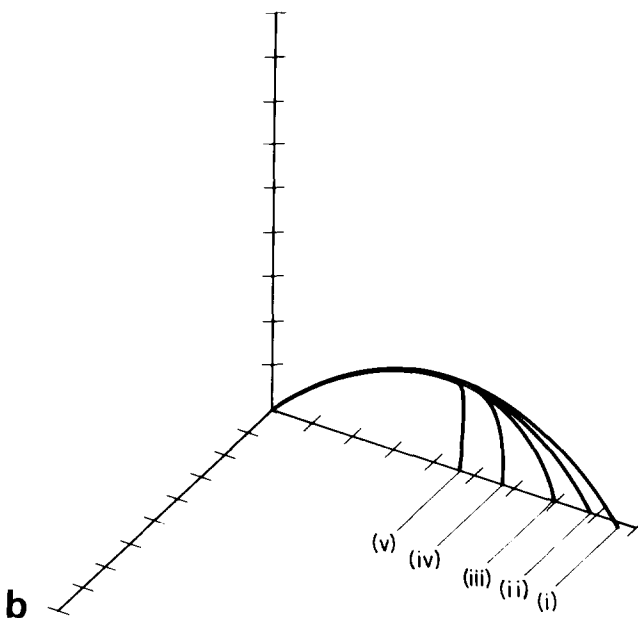
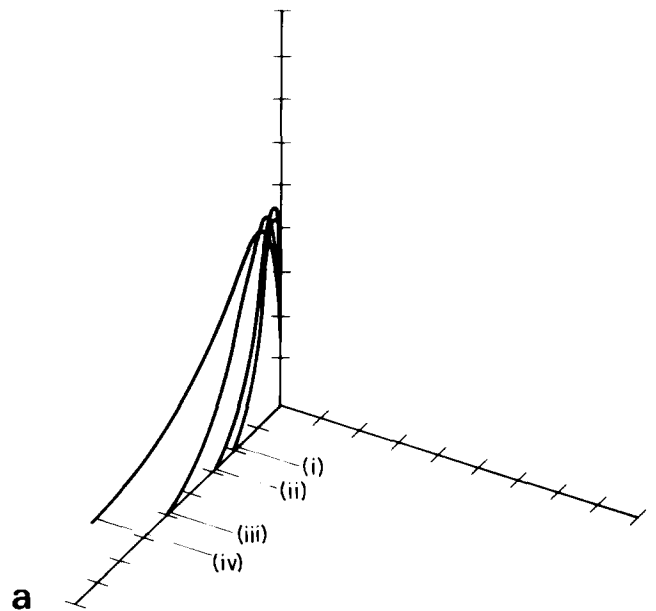
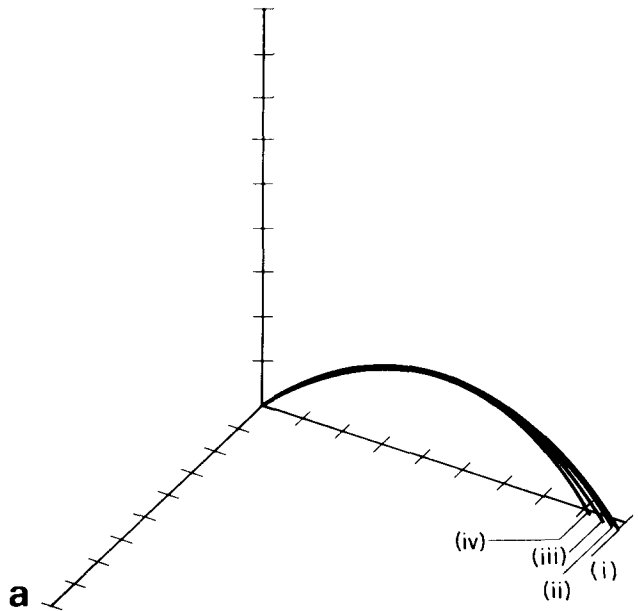


Fig 3 (a) Predicted trajectories using the drag law of  $kV^2(1+AS)$  (one division=25 m) – (i)  $A=0.01$ , (ii)  $A=0.05$ , (iii)  $A=1.0$ , (iv)  $A=50.0$ ; (b) Predicted trajectories using the drag law of  $kV^2(1+e^{bS})$  (one division=25 m) – (i)  $b=0.01$ , (ii)  $b=0.02$ , (iii)  $b=0.03$ , (iv)  $b=0.05$ , (v)  $b=0.10$

Fig 4 (a) Influence of the wind cross drag multiplier  $X$  and decay parameter  $Y$  on vertical jet trajectories (wind 10 m/s, one division=25 m) – (i)  $X=50, Y=0.04$ , (ii)  $X=20, Y=0.02$ , (iii)  $X=50, Y=0.2$ , (iv)  $X=50, Y=0.01$ ; (b) Influence of wind on jet at  $40^\circ$  elevation (wind speed 10 m/s at  $90^\circ$  to jet initial direction, one division=25 m) – (i)  $X=50, Y=0.04$ , (ii)  $X=20, Y=0.02$ , (iii)  $X=50, Y=0.02$ , (iv)  $X=50, Y=0.01$

photographic evidence from which trajectories in still air could be measured. Fig 5, taken for a flow rate of  $2400\text{ m}^3/\text{hr}$ , is typical.

The simulation was fitted to the trajectory at  $40^\circ$  elevation and flow rate  $2400\text{ m}^3/\text{h}$  by changing the parameter  $b$ . For each value of  $b$  the program automatically fits  $k$  to agree with the vertical jet efficiency resulting from the Froude number at the nozzle exit. The closest fit was achieved with  $b=0.023$ .

Using this value the experimental trajectories are compared with predicted trajectories in Fig 6 for flowrates of  $2400$  and  $3600\text{ m}^3/\text{h}$  and for elevations from  $20^\circ$  to  $75^\circ$ .

The measured pressure at the monitor base was 13 bar and the predicted trajectories are based on 12 bar at the nozzle inlet. Throughout this range the simulation gives good agreement. It should also be borne in mind that some error is present in the photographed trajectories since true distance is only reproduced on a photographic plate when the jet is on the centre line of the photographic plate.



Fig 5 Typical water jet (flowrate  $2400 \text{ m}^3/\text{h}$ , nozzle pressure 12.5 bar)

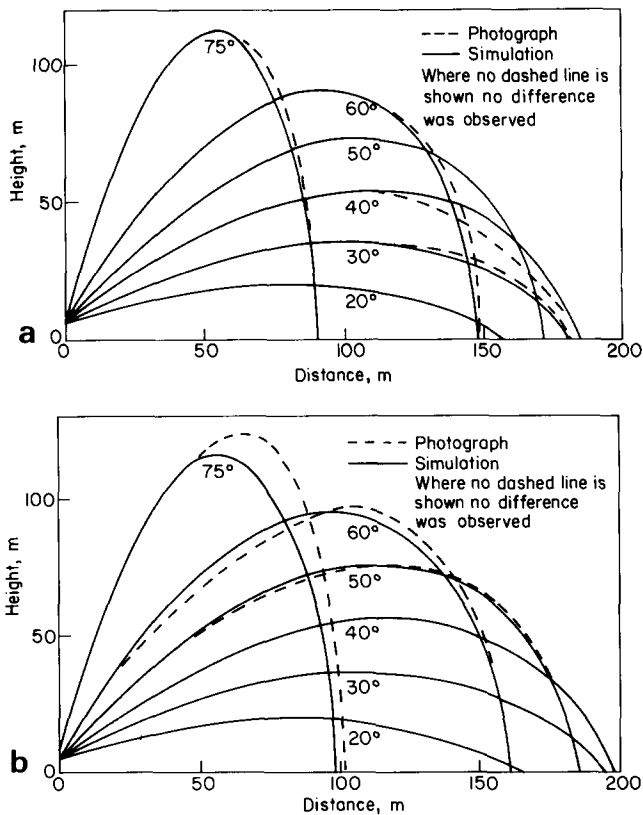


Fig 6 Comparison between computed and photographed trajectories: (a)  $Q = 2400 \text{ m}^3/\text{h}$ ; (b)  $Q = 3600 \text{ m}^3/\text{h}$

### Conclusion

A computer simulation has been proposed which gives good agreement with measured trajectories in still air conditions and provides a useful design aid for predicting jet behaviour in applications such as offshore fire fighting.

The simulation enables the effects of flow rate, pressure, nozzle size, elevation and wind speed on such parameters as power requirement, range and pipework specification to be evaluated. From these data the design parameters for monitor systems to meet the required performance can be laid down.

The mean path of the jet in still air is predicted but not the distribution of jet fall out in the foot print. Since the latter is significantly affected by strong wind speeds there is a need for carefully measured data on the performance of jets in cross winds. If such data were available, greater accuracy of prediction might be readily achievable using the cross jet drag model proposed.

### Acknowledgement

The authors wish to acknowledge the assistance of J. A. Jeffrey in this work.

### References

1. Freeman J. R. Experiments relating to hydraulics of fire streams. *Trans. ASCE*, 1889, **21**, 303–461
2. Rouse H., Howe J. W. and Metzler D. E. Experimental investigation of fire monitors and nozzles. *Proc. ASCE*, 1951, **77**, 29
3. Murakami M. and Katayama K. Discharge coefficients of fire nozzles. *Trans. ASME*, 1966, 706–716
4. Hoyt J. W. and Taylor J. J. Effect of nozzle shape and polymer additives on water jet appearance. *ASME Paper No. 77-FE-16*, 1977
5. Hatton A. P. and Osborne, M. J. The trajectories of large fire fighting jets. *Int. J. Heat & Fluid Flow*, 1979, **1**, 37–41
6. Arato E. G., Crow D. A. and Miller D. S. Investigations of a high performance water nozzle. *BHRA Res. Report 1058*, June 1970
7. Private Communication. Data provided by courtesy of Stang Hydraulics Inc., Worthington European Marine Division and B.P. Shipping